*Inorg. Chem.* **2003**, *42*, 4585–4596

# Cubane-Type Heterometallic Sulfido Clusters: Incorporation of Two Metal Fragments into a Dinuclear $ReS(\mu\text{-}S)_2ReS$ Core Affording Bimetallic $M_2Re_2(\mu_3\text{-}S)_4$ Clusters (M = Ru, Pt, Cu) or Trimetallic $MM'Re_2(\mu_3\text{-}S)_4$ Clusters via Incomplete Cubane-Type $MRe_2(\mu_3\text{-}S)(\mu_2\text{-}S)_3$ Intermediates (M = Ru, Rh, Ir; M′ = Mo, W, Pd, Ru, Rh)

**Hidetake Seino,[†] Tetsuhide Kaneko,[†] Shunpei Fujii,[†] Masanobu Hidai,*[,‡] and Yasushi Mizobe*[,†]**

*Institute of Industrial Science, The University of Tokyo, Komaba, Meguro-ku, Tokyo 153-8505, Japan, and Department of Materials Science and Technology, Faculty of Industrial Science and Technology, Tokyo University of Science, Noda, Chiba 278-8510, Japan*

Received April 14, 2003

Reactions of a dirhenium tetra(sulfido) complex $[PPh_4]_2[ReS(L)(\mu\text{-}S)_2ReS(L)]$ (L = $S_2C_2(SiMe_3)_2$) with a series of group 8–11 metal complexes in MeCN at room temperature afforded either the cubane-type clusters $[\mathbf{M}_2(ReL)_2(\mu_3\text{-}S)_4]$ (**M** = Cp*Ru (**2**), $PtMe_3$, $Cu(PPh_3)$ (**4**); Cp* = $\eta^5$-$C_5Me_5$) or the incomplete cubane-type clusters $[\mathbf{M}(ReL)_2(\mu_3\text{-}S)(\mu_2\text{-}S)_3]$ (**M** = ($\eta^6$-$C_6HMe_5$)Ru (**5**), Cp*Rh (**6**), Cp*Ir (**7**)), depending on the nature of the metal complexes added. It has also been disclosed that the latter incomplete cubane-type clusters can serve as the good precursors to the trimetallic cubane-type clusters still poorly precedented. Thus, treatment of **5**–**7** with a range of metal complexes in THF at room temperature resulted in the formation of novel trimetallic cubane-type clusters, including the neutral clusters $[\{(\eta^6\text{-}C_6HMe_5)Ru\}\{W(CO)_3\}(ReL)_2(\mu_3\text{-}S)_4]$, $[(Cp^*M)\{W(CO)_3\}(ReL)_2(\mu_3\text{-}S)_4]$ (M = Rh, Ir), $[(Cp^*Ir)\{Mo(CO)_3\}(ReL)_2(\mu_3\text{-}S)_4]$, $[\{(\eta^6\text{-}C_6HMe_5)Ru\}\{Pd(PPh_3)\}(ReL)_2(\mu_3\text{-}S)_4]$, and $[(Cp^*Ir)\{Pd(PPh_3)\}(ReL)_2(\mu_3\text{-}S)_4]$ (**13**) along with the cationic clusters $[(Cp^*Ir)(Cp^*Ru)(ReL)_2(\mu_3\text{-}S)_4][PF_6]$ (**14**) and $[(Cp^*Ir)\{Rh(cod)\}(ReL)_2(\mu_3\text{-}S)_4][PF_6]$ (cod = 1,5-cyclooctadiene). The X-ray analyses have been carried out for **2**, **4**, **7**, **13**, and the $SbF_6$ analogue of **14** (**14′**) to confirm their bimetallic cubane-type, bimetallic incomplete cubane-type, or trimetallic cubane-type structures. Fluxional behavior of the incomplete cubane-type and trimetallic cubane-type clusters in solutions has been demonstrated by the variable-temperature $^1H$ NMR studies, which is ascribable to both the metal–metal bond migration in the cluster cores and the pseudorotation of the dithiolene ligand bonded to the square pyramidal Re centers, where the temperatures at which these processes proceed have been found to depend upon the nature of the metal centers included in the cluster cores.

## Introduction

Transition metal−sulfido clusters containing cubane-type $M_4S_4$ cores are currently attracting much attention[1] owing to their relevance to biological[2] and industrial[3] metal sulfide catalysts. A significant number of homo- and heterometallic cubane-type sulfido clusters have already been isolated and characterized in a well-defined manner. Typical examples might be the $Fe_4S_4$[2c,4] and $MoFe_3S_4$[5] clusters as the models of the active sites of ferredoxin and nitrogenase, respectively, as well as the $Mo_2Co_2S_4$ clusters[6] relevant to the possible

* Authors to whom correspondence should be addressed. E-mail: ymizobe@iis.u-tokyo.ac.jp (Y.M.).
† The University of Tokyo.
‡ Tokyo University of Science.

(1) (a) Hidai, M.; Kuwata, S.; Mizobe, Y. *Acc. Chem. Res.* **2000**, *33*, 46. (b) Hernández-Molina, R.; Sokolov, M. N.; Sykes, A. G. *Acc. Chem. Res.* **2001**, *34*, 223. (c) Hernández-Molina, R.; Sykes, A. G. *J. Chem. Soc., Dalton Trans.* **1999**, 3137. (d) Harris, S. *Polyhedron* **1989**, *8*, 2843.

(2) (a) Beinert, H.; Holm, R. H.; Münck, E. *Science* **1997**, *277*, 653. (b) Reviews in *Adv. Inorg. Chem.* **1999**, *47*. (c) Howard, J. B.; Rees, D. C. *Chem. Rev.* **1996**, *96*, 2965.

(3) (a) Lauritsen, J. V.; Helveg, S.; Laegsgaard, E.; Stensgaard, I.; Claussen, B. S.; Topsøe, H.; Besenbacher, F. *J. Catal.* **2001**, *197*, 1. (b) Startsev, A. N. *J. Mol. Catal. A: Chem.* **2000**, *152*, 1. (c) Rakowski Dubois, M. *Chem. Rev.* **1989**, *89*, 1. (d) Brorson, M.; King, J. D.; Kiriakidou, K.; Prestopino, F.; Nordlander, E. In *Metal Clusters in Chemistry*; Braunstein, P., Oro, L. A., Raithby, P. R., Eds.; Wiley-VCH: Weinheim, 1999; Chapter 2.6.

10.1021/ic030129k CCC: $25.00 
Published on Web 06/25/2003

**Scheme 1**

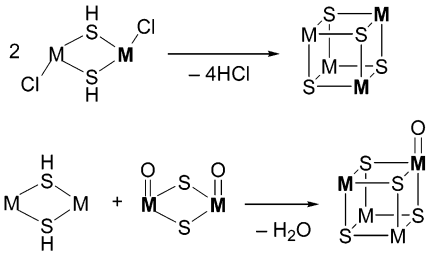

Mo−Co sulfide as the reactive species of the industrial hydrodesulfurization catalyst. We have long been interested in syntheses of a wide range of clusters of these types, especially those with heterobimetallic cores containing noble metals. For this purpose, it is essential to develop rational methods affording the $M_4S_4$ cores with the desired atom composition in high yields.

Our recent studies toward this direction have revealed that hydrosulfido-bridged dinuclear complexes such as [Cp*MCl($\mu$-SH)$_2$MCp*Cl] (M = Ru, Rh, Ir; Cp* = $\eta^5$-$C_5Me_5$) and [Cp$_2$Ti($\mu$-SH)$_2$RuCp*Cl] (Cp = $\eta^5$-$C_5H_5$) serve as versatile precursors for preparing the homo- and heterobimetallic cubane-type clusters such as [(Cp*M)$_4$($\mu_3$-S)$_4$] (M = Ru,[7] Rh, Ir[8]), [(CpTi)$_2$(Cp*Ru)$_2$($\mu_3$-S)$_4$],[9] and [CpTi(Cp*Ru)$_3$($\mu_3$-S)$_4$][10] through a dehydrochlorination−dimerization process (Scheme 1). In addition, it has also been found that the Ir−Mo cluster [(Cp*Ir)$_2${Mo(O)Cl$_2$}{MoCl$_2$(DMF)}($\mu_3$-S)$_4$] can be obtained from [Cp*IrCl($\mu$-SH)$_2$IrCp*Cl] and [MoO(DMF)$_3$($\mu$-S)$_2$MoO(DMF)$_3$]$^{2+}$ through condensation and concomitant dehydration,[11] which is also shown in Scheme 1.

Another potential method to prepare the mixed-metal cubane-type clusters is incorporation of metal fragments into the MS($\mu$-S)$_2$MS templates (M = Mo, W). This method was originally developed by Stiefel and co-workers,[12] and we have applied this methodology to prepare cubane-type clusters containing noble metals. Thus, the reactions of [MS(S$_2$CNEt$_2$)($\mu$-S)$_2$MS(S$_2$CNEt$_2$)] with [Pd(PPh$_3$)$_4$] and [{M′(cod)}$_2$($\mu$-Cl)$_2$] (M′ = Rh, Ir; cod = 1,5-cyclooctadiene)

**Scheme 2**

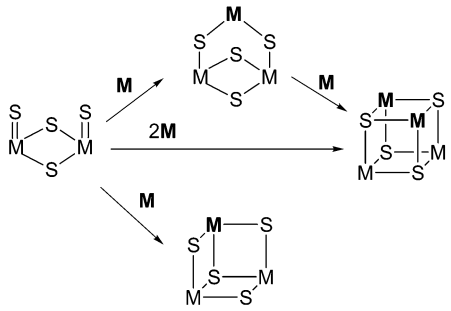

afforded the expected cubane-type clusters [{Mo(S$_2$CNEt$_2$)}$_2$-{Pd(PPh$_3$)}$_2$($\mu_3$-S)$_4$][13] and [{MCl(S$_2$CNEt$_2$)}$_2${M′(cod)}$_2$($\mu_3$-S)$_4$] (Scheme 2).[14] More recently it has turned out that this methodology is applicable to the synthesis of related cubane-type M$_2$Ti$_2$S$_4$ clusters (M = Ru, Rh, Ir, Cu) from [CpTiS($\mu$-S)$_2$Ti(S)Cp]$^{2-}$.[15]

From the reactions of the above MS($\mu$-S)$_2$MS (M = Mo, W) complexes with [M′(PPh$_3$)$_4$] (M′ = Pd, Pt) and [M′Cl(PPh$_3$)$_3$] (M′ = Rh, Ir) under certain conditions, trinuclear tetrakis(sulfido) clusters such as [{M(S$_2$CNEt$_2$)}$_2${M′(PPh$_3$)}($\mu_2$-S)$_4$] (M′ = Pd, Pt)[13] and [{M(S$_2$CNEt$_2$)}$_2${M′(PPh$_3$)$_2$}($\mu_3$-S)($\mu_2$-S)$_3$($\mu_2$-Cl)] (M′ = Rh, Ir)[14] were also available. However, derivatization of trimetallic cubane-type clusters from these trinuclear bimetallic clusters was unsuccessful, although incorporation of the metal fragment into the $M_3S_4$ core giving bimetallic cubane-type $M_3M'S_4$ clusters is well precedented for the reactions of the incomplete cubane-type $Mo_3S_4$ clusters with a series of transition metal and main group metal compounds.[16] Meanwhile, formation of the cubane-type cores from the reactions of the linear M($\mu_2$-S)$_2$M($\mu_2$-S)$_2$M template with a metal fragment is also known: the $Fe_3S_4$ cluster with certain metal complexes and the $VFe_2S_4$ cluster with an Fe complex have been shown to give bimetallic cubane-type $MFe_3S_4$ (e.g., M = Mo, Ni)[17] and $VFe_3S_4$[18] clusters, respectively.

Quite recently, to advance further the chemistry of the MS($\mu$-S)$_2$MS complexes, we have investigated the reactivity of a $Re_2S_4$ complex [PPh$_4$]$_2$[ReS(L)($\mu$-S)$_2$ReS(L)] (**1**; L = S$_2$C$_2$(SiMe$_3$)$_2$)[19] toward various noble metal compounds, which has disclosed that either cubane-type $M_2Re_2S_4$ or the incomplete cubane-type $MRe_2S_4$ clusters are selectively


(4) (a) Holm, R. H.; Ciurli, S.; Weigel, J. A. *Prog. Inorg. Chem.* **1990**, *38*, 1. (b) Berg, J. M.; Holm, R. H. In *Iron-Sulfur Proteins*; Spiro, T. G., Ed.; Wiley-Interscience: New York, 1982; Chapter 1. (c) Lindahl, P. A.; Kovacs, J. A. *J. Cluster Sci.* **1990**, *1*, 29. (d) Beinert, H.; Holm, R. H.; Münck, E. *Science* **1997**, *277*, 653.

(5) (a) Holm, R. H. *Chem. Soc. Rev.* **1981**, *10*, 455. (b) Coucouvanis, D. *Acc. Chem. Res.* **1991**, *24*, 1. (c) Coucouvanis, D.; Demadis, K. D.; Malinak, S. M.; Mosier, P. E.; Tyson, M. A.; Laughlin, L. J. *J. Mol. Catal. A: Chem.* **1996**, *107*, 123. (d) Holm, R. H. *Adv. Inorg. Chem.* **1992**, *38*, 1.

(6) (a) Curtis, M. D.; Druker, S. H. *J. Am. Chem. Soc.* **1997**, *119*, 1027. (b) Mansour, M. A.; Curtis, M. D.; Kampf, J. W. *Organometallics* **1997**, *16*, 3363 and references therein.

(7) (a) Kuwata, S.; Andou, M.; Hashizume, K.; Mizobe, Y.; Hidai, M. *Organometallics* **1998**, *17*, 3429. (b) Hashizume, K.; Mizobe, Y.; Hidai, M. *Organometallics* **1996**, *15*, 3303.

(8) (a) Tang, Z.; Nomura, Y.; Ishii, Y.; Mizobe, Y.; Hidai, M. *Inorg. Chim. Acta* **1998**, *267*, 73. (b) Tang, Z.; Nomura, Y.; Ishii, Y.; Mizobe, Y.; Hidai, M. *Organometallics* **1997**, *16*, 151.

(9) Kabashima, S.; Kuwata, S.; Hidai, M. *J. Am. Chem. Soc.* **1999**, *121*, 7837.

(10) Kabashima, S.; Kuwata, S.; Ueno, K.; Shiro, M.; Hidai, M. *Angew. Chem., Int. Ed.* **2000**, *39*, 1128.

(11) Masumori, T.; Seino, H.; Mizobe, Y.; Hidai, M. *Inorg. Chem.* **2000**, *39*, 5002.

(12) Halbert, T. R.; Cohen, S. A.; Stiefel, E. I. *Organometallics* **1985**, *4*, 1689.

(13) Ikada, T.; Kuwata, S.; Mizobe, Y.; Hidai, M. *Inorg. Chem.* **1998**, *37*, 5793.

(14) Ikada, T.; Kuwata, S.; Mizobe, Y.; Hidai, M. *Inorg. Chem.* **1999**, *38*, 64.

(15) Amemiya, T.; Kuwata, S.; Hidai, M. *Chem. Commun.* **1999**, 711.

(16) (a) Shibahara, T. *Adv. Inorg. Chem.* **1991**, *37*, 143. (b) Shibahara, T.; Sakane, G.; Naruse, Y.; Taya, K.; Akashi, H.; Ichimura, A.; Adachi, H. *Bull. Chem. Soc. Jpn.* **1995**, *68*, 2769. (c) Murata, T.; Mizobe, Y.; Gao, H.; Ishii, Y.; Wakabayashi, T.; Nakano, F.; Tanase, T.; Yano, S.; Hidai, M.; Echizen, I.; Nanikawa, H.; Motomura, S. *J. Am. Chem. Soc.* **1994**, *116*, 3389. (d) Saysell, D. M.; Sokolov, M. N.; Sykes, A. G. In *Transition Metal Sulfur Chemistry*; Stiefel, E. I., Matsumoto, K., Eds.; American Chemical Society: Washington, DC, 1996; Chapter 12.

(17) (a) Coucouvanis, D.; Al-Ahmad, S.; Salifoglou, A.; Dunham, W. R.; Sands, R. H. *Angew. Chem., Int. Ed. Engl.* **1988**, *27*, 1353. (b) Ciurli, S.; Ross, P. K.; Scott, M. J.; Yu, S.-B.; Holm, R. H. *J. Am. Chem. Soc.* **1992**, *114*, 5415.

(18) Kovacs, J. A.; Holm, R. H. *Inorg. Chem.* **1987**, *26*, 702.

(19) Goodman, J. T.; Rauchfuss, T. B. *Inorg. Chem.* **1998**, *37*, 5040.

**Scheme 3**

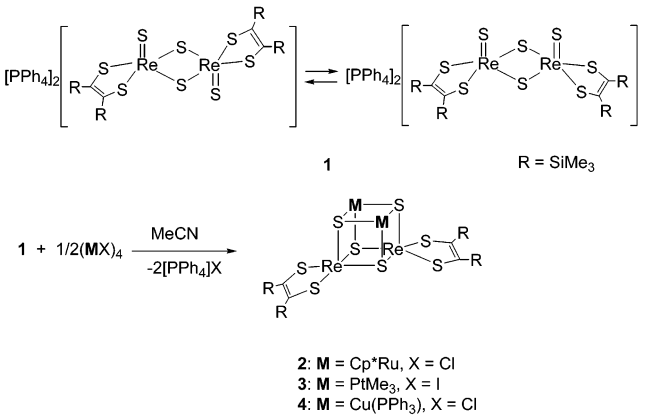


formed depending on the nature of the heterometal (M) compounds employed. Furthermore, it has turned out that trimetallic cubane-type $MM'Re_2S_4$ clusters are readily available from the latter incomplete cubane-type clusters. In this paper, we wish to describe the details of a series of these new bi- and trimetallic cubane-type and incomplete cubane-type clusters derived from the dirhenium complex **1**. These results indicate that the incorporation of two metal fragments into the dinuclear tetrakis(sulfido) cores $MS(\mu\text{-}S)_2MS$ also provides quite a versatile method to construct various cubane-type cores not only for M = Mo, W, and Ti as demonstrated previously but also for M = Re. It should be emphasized that the rational synthesis of a series of trimetallic cubane-type clusters has been attained for the first time by starting from **1**.

## Results and Discussion

**Reactions Affording Bimetallic Cubane-Type $M_2Re_2(\mu_3\text{-}S)_4$ Clusters from 1.** Treatment of **1** with a series of metal complexes such as $[(Cp^*Ru)_4(\mu_3\text{-}Cl)_4]$, $[(PtMe_3)_4(\mu_3\text{-}I)_4]$, and $[\{Cu(PPh_3)\}_4(\mu_3\text{-}Cl)_4]$ (0.5 equiv; M:Re = 1:1) in MeCN at room temperature resulted in the precipitation of solids, which were collected and crystallized from THF−MeCN to give the analytically pure crystals of bimetallic cubane-type $M_2Re_2(\mu_3\text{-}S)_4$ clusters $[(Cp^*Ru)_2(ReL)_2(\mu_3\text{-}S)_4]$ (**2**), $[(PtMe_3)_2(ReL)_2(\mu_3\text{-}S)_4]$ (**3**), and $[\{Cu(PPh_3)\}_2(ReL)_2(\mu_3\text{-}S)_4]$ (**4**), respectively (Scheme 3).[20]

Clusters **2**−**4** were characterized by elemental analyses as well as spectroscopic data, and the structures were determined in detail by the X-ray analyses for **2** and **4** as described below. Preliminary X-ray diffraction study for **3** has also disclosed the formation of the expected cubane-type $Pt_2Re_2(\mu_3\text{-}S)_4$ core. For all clusters **2**−**4**, the signals due to the $SiMe_3$ protons appear as one singlet in their $^1H$ NMR spectra, indicating that the four $SiMe_3$ groups in the dithiolene ligands are all equivalent for these clusters in solution because of the presence of two pseudo mirror planes bisecting either the Re−Re or M−M (M = Ru, Pt, or Cu) vector.

(20) Complex **1** is known to have a centrosymmetric trans structure in a solid state, which isomerizes into a cis derivative to give an equilibrated mixture in solution.[19]

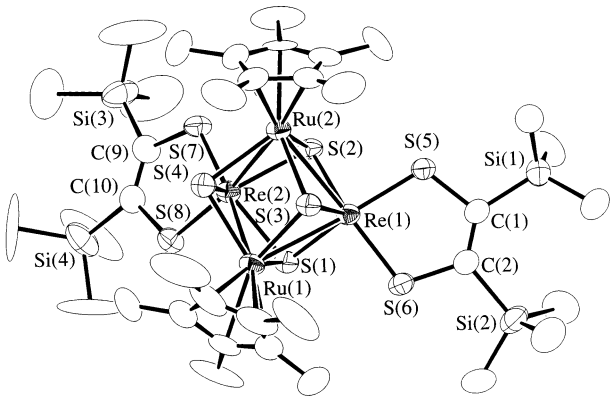


**Figure 1.** An ORTEP drawing of molecule 1 in **2**. Hydrogen atoms are omitted for clarity.

**X-ray Structures of 2 and 4.** The asymmetric unit in the single crystal of **2** contains two independent molecules, whose structures are essentially identical. An ORTEP drawing of one molecule is shown in Figure 1, while the important bonding parameters in two molecules are listed in Table 1. For each of the $Ru_2Re_2$ cores in molecules 1 and 2, there exist four metal−metal bonds between the Ru and Re atoms whose distances fall in the range 2.919(1)−2.941(1) Å in the former and 2.922(1)−2.947(1) Å in the latter, whereas the Re−Re separations of 3.3729(8) and 3.3858(7) Å as well as the Ru−Ru separations of 3.543(1) and 3.529(1) Å are indicative of the absence of any bonding interactions between these atoms. If the dithiolene ligand $L^{2-}$ is considered as a 4e donor, the sum of the electron count around four metal centers is 68 even after taking the four Re−Ru single bonds into account. This value is 4e short from the ideal 72 electrons expected for the four 18e metal centers. The nearly planar feature of the $ReS_2C_2$ rings as well as relatively short $Re-S_{dithiolene}$ bond distances (vide infra) in **2** presumably indicates the presence of the concomitant $\pi$-donation of the lone-pair electron densities from the S atoms in the $L^{2-}$ ligands.

Four faces of this distorted $Ru_2Re_2$ tetrahedron were each capped by a $\mu_3$-S ligand. If the Ru−Re bonds are ignored, the Ru atoms have a three-legged piano stool structure, while the geometry around the Re centers is square pyramidal with the S(3) and S(4) atoms in molecule 1 and the S(11) and S(12) atoms in molecule 2 at the apical positions. Among the three $Re-S_{sulfido}$ bonds around each Re atom, that associated with the apical sulfido atom (2.21−2.23 Å) is shorter than the other two sulfido atoms in the basal plane (2.34−2.37 Å), although the former is elongated significantly from the Re=S bond length in the parent complex **1** (2.123(2) Å).[19] It is to be noted that the two Re−S bonds relating to the dithiolene S atoms (2.25−2.27 Å) are somewhat shorter than the $Re-S_{sulfido}$ bonds for the S atoms in the basal plane, which is the feature observed also in **1**. As for the three Ru−S bonds for each Ru atom, those involving the S atoms bonded further to two Re atoms are shorter than the other two. With respect to the angles around the sulfido atoms, the Ru−S−Ru and Re−S−Re angles (91−97°) are much wider than the Ru−S−Re angles varying from 77° to 80°, because the Ru−Ru and Re−Re separations are longer

**Table 1.** Selected Bond Distances and Angles in **2**

(a) Bond Distances (Å)

| | | | |
|---|---|---|---|
| Molecule 1 | | | |
| Re(1)−Ru(1) | 2.919(1) | Re(1)−Ru(2) | 2.933(1) |
| Re(2)−Ru(1) | 2.941(1) | Re(2)−Ru(2) | 2.929(1) |
| Re(1)−S(1) | 2.357(3) | Re(1)−S(2) | 2.347(4) |
| Re(1)−S(3) | 2.220(4) | Re(1)−S(5) | 2.256(3) |
| Re(1)−S(6) | 2.260(4) | Re(2)−S(1) | 2.347(4) |
| Re(2)−S(2) | 2.365(3) | Re(2)−S(4) | 2.211(5) |
| Re(2)−S(7) | 2.260(4) | Re(2)−S(8) | 2.253(3) |
| Ru(1)−S(1) | 2.319(5) | Ru(1)−S(3) | 2.372(3) |
| Ru(1)−S(4) | 2.395(4) | Ru(2)−S(2) | 2.313(4) |
| Ru(2)−S(3) | 2.378(4) | Ru(2)−S(4) | 2.393(3) |
| Re(1)···Re(2) | 3.3729(8) | Ru(1)···Ru(2) | 3.543(1) |
| Molecule 2 | | | |
| Re(3)−Ru(3) | 2.925(1) | Re(3)−Ru(4) | 2.941(1) |
| Re(4)−Ru(3) | 2.947(1) | Re(4)−Ru(4) | 2.922(1) |
| Re(3)−S(9) | 2.348(3) | Re(3)−S(10) | 2.360(3) |
| Re(3)−S(11) | 2.218(4) | Re(3)−S(13) | 2.256(3) |
| Re(3)−S(14) | 2.260(4) | Re(4)−S(9) | 2.344(4) |
| Re(4)−S(10) | 2.362(3) | Re(4)−S(12) | 2.227(4) |
| Re(4)−S(15) | 2.269(3) | Re(4)−S(16) | 2.251(3) |
| Ru(3)−S(9) | 2.314(4) | Ru(3)−S(11) | 2.382(3) |
| Ru(3)−S(12) | 2.405(4) | Ru(4)−S(10) | 2.314(4) |
| Ru(4)−S(11) | 2.382(3) | Ru(4)−S(12) | 2.376(3) |
| Re(3)···Re(4) | 3.3858(7) | Ru(3)···Ru(4) | 3.529(1) |

(b) Bond Angles (deg)

| | | | |
|---|---|---|---|
| Molecule 1 | | | |
| S(1)−Re(1)−S(2) | 78.8(1) | S(1)−Re(1)−S(3) | 102.9(1) |
| S(1)−Re(1)−S(5) | 146.1(2) | S(1)−Re(1)−S(6) | 88.0(1) |
| S(2)−Re(1)−S(3) | 102.7(1) | S(2)−Re(1)−S(5) | 88.1(1) |
| S(2)−Re(1)−S(6) | 143.0(2) | S(3)−Re(1)−S(5) | 110.5(1) |
| S(3)−Re(1)−S(6) | 114.0(2) | S(5)−Re(1)−S(6) | 83.9(1) |
| S(1)−Re(2)−S(2) | 78.6(1) | S(1)−Re(2)−S(4) | 103.1(1) |
| S(1)−Re(2)−S(7) | 143.9(2) | S(1)−Re(2)−S(8) | 89.7(1) |
| S(2)−Re(2)−S(4) | 103.1(1) | S(2)−Re(2)−S(7) | 87.5(1) |
| S(2)−Re(2)−S(8) | 146.4(2) | S(4)−Re(2)−S(7) | 112.5(2) |
| S(4)−Re(2)−S(8) | 110.3(1) | S(7)−Re(2)−S(8) | 83.8(1) |
| S(1)−Ru(1)−S(3) | 99.5(1) | S(1)−Ru(1)−S(4) | 98.5(1) |
| S(3)−Ru(1)−S(4) | 76.9(1) | S(2)−Ru(2)−S(3) | 99.0(1) |
| S(2)−Ru(2)−S(4) | 99.2(1) | S(3)−Ru(2)−S(4) | 76.9(1) |
| Molecule 2 | | | |
| S(9)−Re(3)−S(10) | 78.4(1) | S(9)−Re(3)−S(11) | 102.9(1) |
| S(9)−Re(3)−S(13) | 146.9(2) | S(9)−Re(3)−S(14) | 86.4(1) |
| S(10)−Re(3)−S(11) | 102.5(1) | S(10)−Re(3)−S(13) | 90.8(1) |
| S(10)−Re(3)−S(14) | 142.6(2) | S(11)−Re(3)−S(13) | 110.0(1) |
| S(11)−Re(3)−S(14) | 114.2(1) | S(13)−Re(3)−S(14) | 83.5(1) |
| S(9)−Re(4)−S(10) | 78.5(1) | S(9)−Re(4)−S(12) | 102.9(1) |
| S(9)−Re(4)−S(15) | 141.8(2) | S(9)−Re(4)−S(16) | 87.4(1) |
| S(10)−Re(4)−S(12) | 102.9(1) | S(10)−Re(4)−S(15) | 89.1(1) |
| S(10)−Re(4)−S(16) | 146.2(2) | S(12)−Re(4)−S(15) | 115.0(1) |
| S(12)−Re(4)−S(16) | 110.2(1) | S(15)−Re(4)−S(16) | 83.3(1) |
| S(9)−Ru(3)−S(11) | 99.0(1) | S(9)−Ru(3)−S(12) | 98.5(1) |
| S(11)−Ru(3)−S(12) | 77.2(1) | S(10)−Ru(4)−S(11) | 99.0(1) |
| S(10)−Ru(4)−S(12) | 99.9(1) | S(11)−Ru(4)−S(12) | 77.7(1) |

than the Ru−Re distances. Figure 1 as well as the metric data in Table 1 shows the presence of two pseudo mirror planes, one being defined by two Ru and two sulfido atoms and the other by two Re atoms and the remaining two sulfido atoms, which is consistent with the $^1$H NMR data described above.

It is also interesting to note that, in the single crystal, six molecules of **2** that are crystallographically equivalent and mutually related by either an inversion or a $C_3$ operation are assembling in a cyclic manner as indicated in Figure 2. Weak interaction might be present between one of the two Cp* rings of the given molecule and the two $S_{sulfido}$ atoms of the $Re_2S_2$ ring in the neighboring molecule, where the distances

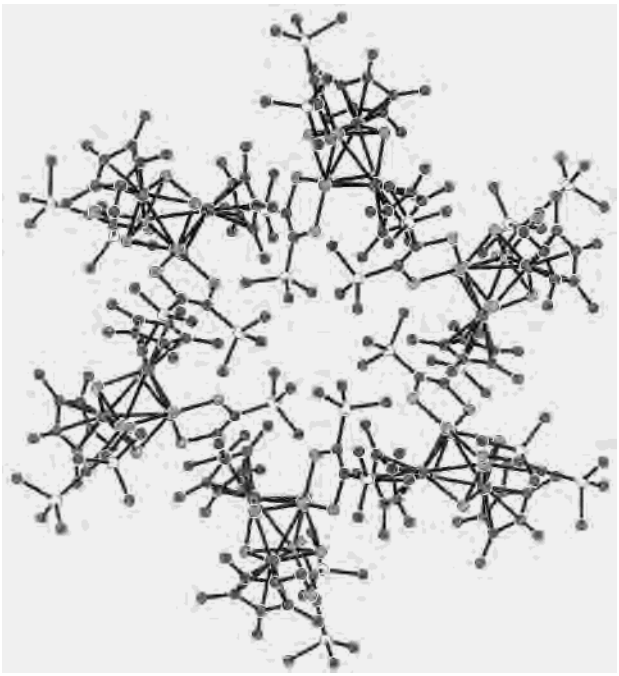

**Figure 2.** Assembly of six crystallographically equivalent molecules of **2** via interactions between the Cp* plane and the $Re_2S_2$ face of the cubane core.

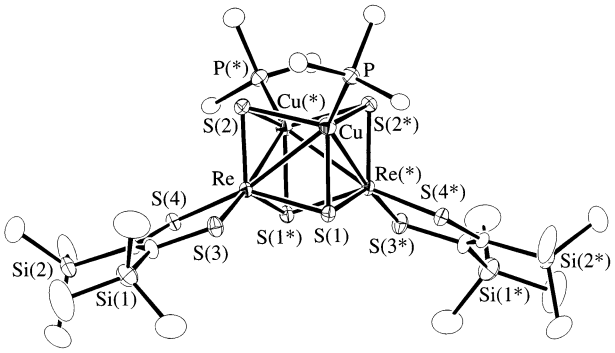


**Figure 3.** An ORTEP drawing of **4**. The phenyl carbons except for those at the ipso positions and all hydrogen atoms are omitted for clarity.

between the cyclopentadienyl C atoms and the S atoms are in the ranges 3.70(2)−4.26(3) and 3.56(1)−4.35(2) Å for molecules 1 and 2, respectively.

Figure 3 depicts the ORTEP drawing of **4**; the selected bond distances and angles in **4** are collected in Table 2. The molecule contains two tetrahedral Cu centers as well as the two square pyramidal Re centers, and it has a crystallographic $C_2$ axis passing through the midpoints of both the Cu−Cu and Re−Re vectors in the $Cu_2Re_2$ core. The formal electron count for **4** is the same as that for **2** in consideration of the presence of four Cu−Re single bonds with the length at 2.821(1) or 2.808(1) Å. The Re−Re and Cu−Cu separations at 3.4308(8) and 3.067(2) Å, respectively, correspond to those without any bonding interaction. Other structural features are in good agreement with those in **2**.

**Reactions Affording Incomplete Cubane-Type $MRe_2$-($\mu_3$-S)($\mu_2$-S)$_3$ Clusters from 1.** When [{($\eta^6$-$C_6HMe_5$)RuCl}$_2$-($\mu$-Cl)$_2$] or [(Cp*MCl)$_2$($\mu$-Cl)$_2$] (M = Rh, Ir) were reacted with **1** in MeCN at room temperature in the atomic ratio of heterometal:Re = 1/2, incomplete cubane-type clusters

**Table 2.** Selected Bond Distances and Angles in **4**

(a) Bond Distances (Å)

| | | | |
|---|---|---|---|
| Re−Cu | 2.821(1) | Re−Cu* | 2.808(1) |
| Re−S(1) | 2.374(2) | Re−S(1*) | 2.362(2) |
| Re−S(2) | 2.185(2) | Re−S(3) | 2.256(2) |
| Re−S(4) | 2.261(2) | Cu−S(1) | 2.277(2) |
| Cu−S(2) | 2.417(2) | Cu−S(2*) | 2.433(3) |
| Cu−P | 2.234(2) | | |
| Re···Re* | 3.4308(8) | Cu···Cu* | 3.067(2) |

(b) Bond Angles (deg)

| | | | |
|---|---|---|---|
| S(1)−Re−S(1*) | 78.23(8) | S(1)−Re−S(2) | 107.14(8) |
| S(1)−Re−S(3) | 86.49(8) | S(1)−Re−S(4) | 142.77(7) |
| S(1*)−Re−S(2) | 108.09(8) | S(1*)−Re−S(3) | 138.62(8) |
| S(1*)−Re−S(4) | 86.53(7) | S(2)−Re−S(3) | 113.14(9) |
| S(2)−Re−S(4) | 109.85(8) | S(3)−Re−S(4) | 82.91(8) |
| S(1)−Cu−S(2) | 102.79(8) | S(1)−Cu−S(2*) | 102.77(8) |
| S(1)−Cu−P | 127.44(10) | S(2)−Cu−S(2*) | 95.28(8) |
| S(2)−Cu−P | 111.13(9) | S(2*)−Cu−P | 112.41(9) |

[{($\eta^6$-$C_6HMe_5$)Ru}$(ReL)_2(\mu_3$-S)($\mu_2$-S)$_3$] (**5**) and [(Cp*M)-$(ReL)_2(\mu_3$-S)($\mu_2$-S)$_3$] (M = Rh (**6**), Ir (**7**)) precipitated (eq 1), which were filtered off and crystallized from THF−MeCN. The products **5**−**7** were characterized spectroscopically and by elemental analyses. An X-ray diffraction study has been undertaken for **7** to confirm its incomplete cubane-type structure (vide infra). An increase in the atomic ratio of heterometal:Re up to 1 also afforded the reaction mixtures containing these incomplete cubane-type clusters as the only isolable product; neither the cubane-type $M_2Re_2$ clusters nor any other tractable metal-containing products were isolated. Thus, under the conditions employed, all of the reactions shown in Scheme 3 and eq 1 proceed in such a manner that the neutral clusters are produced with concomitant formation of 2 equiv of [$PPh_4$]X (X = Cl or I). Since these neutral clusters are sparingly soluble in polar MeCN, the reactions presumably terminate upon precipitation of these products. The choice of the core structure therefore depends upon the charge of the metal fragment incorporated to the $Re_2S_4$ template: viz., the monocationic unit leads to the $M_2Re_2$ core, while the dicationic chromophore results in the $MRe_2$ cluster.

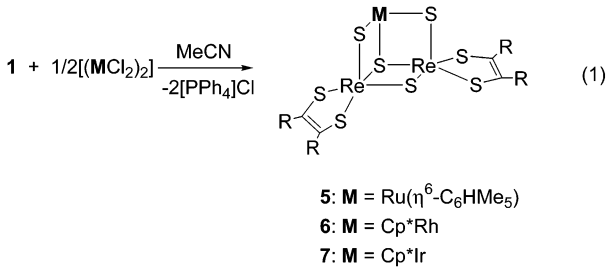


**5**: **M** = Ru($\eta^6$-$C_6HMe_5$)
**6**: **M** = Cp*Rh
**7**: **M** = Cp*Ir

**X-ray Structure of 7.** An X-ray analysis has disclosed unambiguously the incomplete cubane-type core of **7** containing an open triangular $IrRe_2$ core with one $\mu_3$-S and three $\mu_2$-S ligands, which is shown in Figure 4. Important bonding parameters are summarized in Table 3. Cluster **7** has a crystallographic mirror plane defined by Ir, S(1), and S(2) atoms. The Ir−Re distance at 2.918(1) Å is consistent with the presence of the metal−metal single bond, whereas the Re−Re separation of 3.285(1) Å might suggest the absence of bonding interaction, although it is considerably shorter than those in **1** (3.657 Å), **2** (3.3729(8) and 3.3858(7) Å), and **4** (3.4308(8) Å).

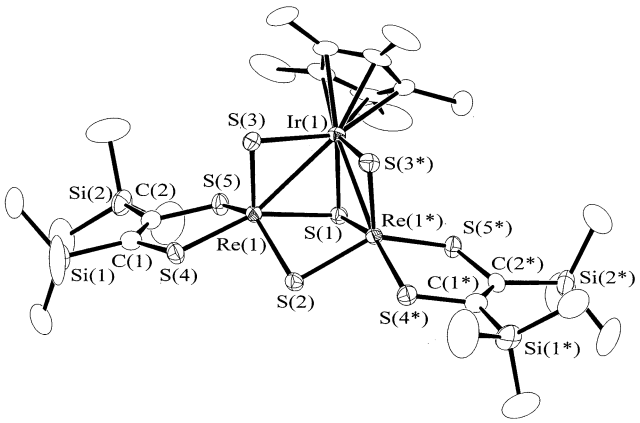


**Figure 4.** An ORTEP drawing of **7**. Hydrogen atoms are omitted for clarity.

**Table 3.** Selected Bond Distances and Angles in **7**

(a) Bond Distances (Å)

| | | | |
|---|---|---|---|
| Ir−Re | 2.918(1) | Ir−S(1) | 2.343(5) |
| Ir−S(3) | 2.397(4) | Re−S(1) | 2.374(4) |
| Re−S(2) | 2.326(3) | Re−S(3) | 2.182(4) |
| Re−S(4) | 2.267(4) | Re−S(5) | 2.252(4) |
| Re···Re* | 3.285(1) | | |

(b) Bond Angles (deg)

| | | | |
|---|---|---|---|
| S(1)−Ir−S(3) | 99.4(1) | S(3)−Ir−S(3*) | 83.9(2) |
| S(1)−Re−S(2) | 78.8(2) | S(1)−Re−S(3) | 105.0(2) |
| S(1)−Re−S(4) | 150.5(2) | S(1)−Re−S(5) | 87.2(1) |
| S(2)−Re−S(3) | 111.7(2) | S(2)−Re−S(4) | 88.1(1) |
| S(2)−Re−S(5) | 135.3(2) | S(3)−Re−S(4) | 104.4(2) |
| S(3)−Re−S(5) | 112.9(2) | S(4)−Re−S(5) | 83.7(2) |

The Ir atom has a three-legged piano stool structure with the $\mu_2$-S(3)−Ir−$\mu_2$-S(3*) angle (83.9(2)°) being smaller than the $\mu_3$-S(1)−Ir−$\mu_2$-S(3) angle (99.4(1)°), while the geometry around the Re atoms is square pyramidal. The distance of the Re center from the apical S(3) atom at 2.182(4) Å is significantly shorter than those from the other $S_{sulfido}$ atoms, $\mu_2$-S(2) and the $\mu_3$-S(1), of 2.326(3) and 2.374(4) Å, respectively. With respect to the angles around the S atoms, the M−S−M linkages bridging two bonded metals have the smaller M−S−M angles; the Ir−$\mu_3$-S(1)−Re and Re−$\mu_3$-S(1)−Re* angles are 76.4(2)° and 87.6(2)°, and the Ir−$\mu_2$-S(3)−Re and Re−$\mu_2$-S(2)−Re* angles are 79.0(1)° and 89.8(2)°, respectively. The presence of the planar dithiolene rings and relatively short Re−$S_{dithiolene}$ bonds is the feature observed also in **2** and **4**.

**Preparation of Trimetallic Cubane-Type MM′$Re_2(\mu_3$-S)$_4$ Clusters from 5−7.** Importantly, it has been disclosed that the incomplete cubane-type clusters obtained here can serve as good precursors to synthesize novel trimetallic cubane-type MM′$Re_2(\mu_3$-S)$_4$ clusters. Thus, the reactions of **5**, **6**, or **7** with a stoichiometric amount of [M(CO)$_3$(MeCN)$_3$] (M = W, Mo), [Pd($PPh_3$)$_4$], and [Cp*Ru(MeCN)$_3$][$PF_6$], as well as a mixture of 0.5 equiv of [{Rh(cod)}$_2(\mu$-Cl)$_2$] and $KPF_6$ in THF, afforded neutral or cationic clusters such as [{($\eta^6$-$C_6HMe_5$)Ru}{W(CO)$_3$}$(ReL)_2(\mu_3$-S)$_4$] (**8**), [(Cp*M)-{W(CO)$_3$}$(ReL)_2(\mu_3$-S)$_4$] (M = Rh (**9**), Ir (**10**)), [(Cp*Ir)-{Mo(CO)$_3$}$(ReL)_2(\mu_3$-S)$_4$] (**11**), [($\eta^6$-$C_6HMe_5$)Ru}{Pd($PPh_3$)}-$(ReL)_2(\mu_3$-S)$_4$] (**12**), [(Cp*Ir){Pd($PPh_3$)}$(ReL)_2(\mu_3$-S)$_4$] (**13**), [(Cp*Ir)(Cp*Ru)$(ReL)_2(\mu_3$-S)$_4$][$PF_6$] (**14**), and [(Cp*Ir){Rh-

**Scheme 4**

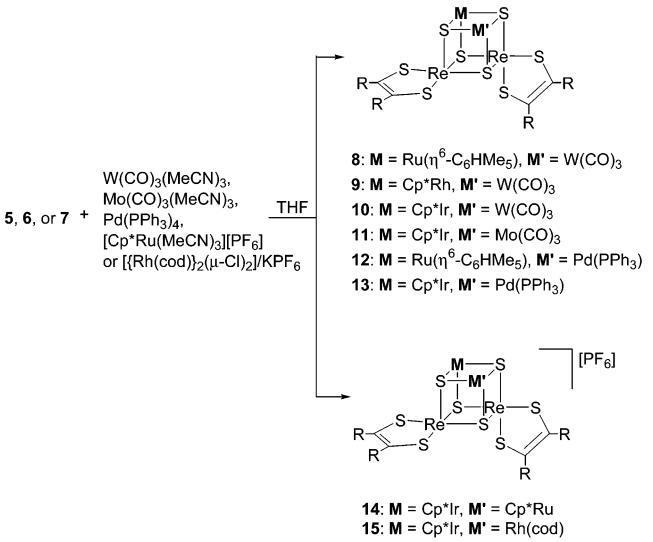


(cod)}$(ReL)_2(\mu_3\text{-}S)_4][PF_6]$ (**15**) (Scheme 4). Unambiguous characterization of the cubane-type core by X-ray analysis was successful for **13** along with the $SbF_6$ analogue of **14** (**14′**). It is noteworthy that the stepwise incorporation of two different metal fragments into the $ReS(\mu\text{-}S)_2ReS$ template reported here provides a versatile method to synthesize a variety of trimetallic cubane-type clusters. Application of such synthetic pathways to the construction of trimetallic cubane-type cores is quite rare; to our knowledge, synthesis of two $Mo_2WCuS_4$ clusters by reacting $[MoS(S_2PR_2)(\mu\text{-}S)_2\text{-}MoS(S_2PR_2)]$ (R = Et, $Pr^n$) first with $[W(CO)_3(MeCN)_3]$ and then with CuI might be the sole precedented example, for which, however, the intermediate $Mo_2WS_4$ clusters were not characterized in a well-defined manner.[21] It is to be noted that trimetallic cubane-type clusters prepared by replacement of one metal atom in the bimetallic cubane-type cores are known: $[\{(MeCp)V\}_2\{Fe(NO)\}\{Co(NO)\}(\mu_3\text{-}S)_4]$ from $[\{(MeCp)V\}_2\{Fe(NO)\}_2(\mu_3\text{-}S)_4]$ with $[Co(NO)(CO)_3]$ (MeCp = $\eta^5$-$C_5H_4Me$)[22] and $[(Cp^*Mo)_2\{Fe(NO)\}(CuCl)(\mu_3\text{-}S)_4]$ from $[(Cp^*Mo)_2(CuCl)_2(\mu_3\text{-}S)_4]$ with $[Fe(NO)(CO)_3]$.[23]

Clusters **8**−**11** containing the "$M(CO)_3$" fragment showed three characteristic $\nu(C{\equiv}O)$ bands in the regions 2004−1890 $cm^{-1}$ for M = W and 2007−1908 $cm^{-1}$ for M = Mo in their IR spectra. These values are significantly higher than those of the parent $[M(CO)_3(MeCN)_3]$ (M = W, 1904 and 1786 $cm^{-1}$; M = Mo, 1913 and 1776 $cm^{-1}$), indicating the presence of much weaker electron back-donation toward the CO ligands from the W and Mo centers incorporated into the corner of these cubane-type cores than that in the parent M(0) complexes. Among the three clusters containing the "$W(CO)_3$" unit, back-donating ability of the W center decreases in the order **8** > **10** > **9**, which are the clusters consisting of the ($\eta^6$-$C_6HMe_5$)Ru, Cp*Ir, and Cp*Rh sites, respectively.

(21) Diller, H.; Keck, H.; Wunderlich, H.; Kuchen, W. *J. Organomet. Chem.* **1995**, *489*, 123.
(22) Rauchfuss, T. B.; Weatherill, T. D.; Wilson, S. R.; Zebrowski, J. P. *J. Am. Chem. Soc.* **1983**, *105*, 6508.
(23) Brunner, H.; Grassl, R.; Wachter, J.; Nuber, B.; Ziegler, M. L. *J. Organomet. Chem.* **1990**, *393*, 119.

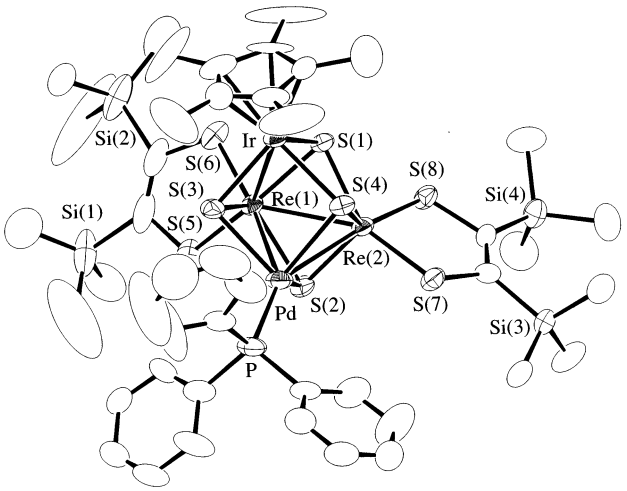


**Figure 5.** An ORTEP drawing of **13**. Hydrogen atoms are omitted for clarity.

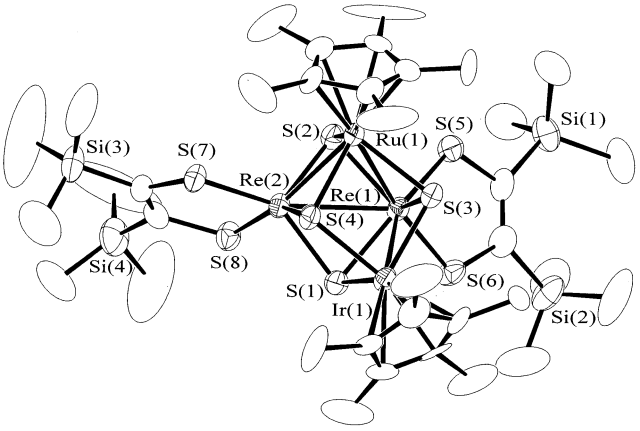


**Figure 6.** An ORTEP drawing of the cation in **14′**. For the disordered Cp* ligands, only those with higher occupancies are shown. Hydrogen atoms are omitted for clarity.

**X-ray Structures of 13 and 14′.** The ORTEP drawings of **13** and **14′** are shown in Figures 5 and 6, which clearly indicate the presence of the trimetallic cubane-type cores in these clusters. Important bond distances and angles are listed in Tables 4 and 5.

As observed for **2** and **4**, the sum of the electron counts around four metals in **13** and **14′** are 68 when the $L^{2-}$ ligands are each tentatively regarded as the 4-electron donor, given the presence of the four metal−metal single bonds. Thus, the separations between two heterometals incorporated into the $Re_2$ core correspond to the nonbonding distances (**13**, Ir−Pd, 3.529(1); **14′**, Ir−Ru, 3.588(5) Å) as observed in **2** and **4**. However, in contrast to **2** and **4**, there exists a Re−Re single bond (**13**, 2.827(1); **14′**, 2.899(3) Å) and alternatively one Re−Ir distance among the four Re−heterometal distances is that without bonding interactions (Ir−Re(2), 3.5354(8) for **13**, 3.563(3) Å for **14′**). Hence, two five-coordinate Re centers with a square pyramidal geometry are no longer equivalent, which presents a striking contrast to the structures observed for the bimetallic cubane-type clusters **2** and **4**. The Ir atoms have a three-legged piano stool structure if the metal−metal bondings are ignored, while the

**Table 4.** Selected Bond Distances and Angles in **13**

(a) Bond Distances (Å)

| | | | |
|---|---|---|---|
| Ir−Re(1) | 2.8658(8) | Re(1)−Re(2) | 2.827(1) |
| Re(1)−Pd | 2.814(2) | Re(2)−Pd | 2.837(1) |
| Ir−S(1) | 2.321(4) | Ir−S(3) | 2.341(4) |
| Ir−S(4) | 2.392(4) | Re(1)−S(1) | 2.327(4) |
| Re(1)−S(2) | 2.391(4) | Re(1)−S(3) | 2.205(4) |
| Re(1)−S(5) | 2.308(4) | Re(1)−S(6) | 2.291(4) |
| Re(2)−S(1) | 2.328(4) | Re(2)−S(2) | 2.245(4) |
| Re(2)−S(4) | 2.343(4) | Re(2)−S(7) | 2.288(4) |
| Re(2)−S(8) | 2.273(4) | Pd−S(2) | 2.340(4) |
| Pd−S(3) | 2.411(4) | Pd−S(4) | 2.524(4) |
| Pd−P | 2.287(5) | | |
| Ir···Re(2) | 3.5354(8) | Ir···Pd | 3.529(1) |

(b) Bond Angles (deg)

| | | | |
|---|---|---|---|
| S(1)−Ir−S(3) | 100.5(1) | S(1)−Ir−S(4) | 78.4(1) |
| S(3)−Ir−S(4) | 87.4(1) | S(1)−Re(1)−S(2) | 101.0(1) |
| S(1)−Re(1)−S(3) | 104.5(1) | S(1)−Re(1)−S(5) | 155.3(2) |
| S(1)−Re(1)−S(6) | 82.1(2) | S(2)−Re(1)−S(3) | 106.9(1) |
| S(2)−Re(1)−S(5) | 80.4(2) | S(2)−Re(1)−S(6) | 141.5(2) |
| S(3)−Re(1)−S(5) | 98.6(2) | S(3)−Re(1)−S(6) | 109.5(2) |
| S(5)−Re(1)−S(6) | 82.0(2) | S(1)−Re(2)−S(2) | 105.4(1) |
| S(1)−Re(2)−S(4) | 79.2(1) | S(1)−Re(2)−S(7) | 150.5(1) |
| S(1)−Re(2)−S(8) | 85.7(1) | S(2)−Re(2)−S(4) | 110.3(1) |
| S(2)−Re(2)−S(7) | 104.0(1) | S(2)−Re(2)−S(8) | 115.2(2) |
| S(4)−Re(2)−S(7) | 89.3(1) | S(4)−Re(2)−S(8) | 134.4(2) |
| S(7)−Re(2)−S(8) | 83.2(1) | S(2)−Pd−S(3) | 102.0(1) |
| S(2)−Pd−S(4) | 101.4(1) | S(2)−Pd−P | 129.4(2) |
| S(3)−Pd−S(4) | 83.0(1) | S(3)−Pd−P | 109.2(2) |
| S(4)−Pd−P | 120.8(2) | | |

**Table 5.** Selected Bond Distances and Angles in **14′**

(a) Bond Distances (Å)

| | | | |
|---|---|---|---|
| Ir−Re(1) | 2.885(3) | Re(1)−Re(2) | 2.899(3) |
| Re(1)−Ru | 2.878(5) | Re(2)−Ru | 2.875(5) |
| Ir−S(1) | 2.33(2) | Ir−S(3) | 2.34(1) |
| Ir−S(4) | 2.40(1) | Re(1)−S(1) | 2.35(1) |
| Re(1)−S(2) | 2.35(1) | Re(1)−S(3) | 2.24(1) |
| Re(1)−S(5) | 2.29(1) | Re(1)−S(6) | 2.30(2) |
| Re(2)−S(1) | 2.34(1) | Re(2)−S(2) | 2.24(1) |
| Re(2)−S(4) | 2.37(1) | Re(2)−S(7) | 2.27(1) |
| Re(2)−S(8) | 2.27(2) | Ru−S(2) | 2.32(2) |
| Ru−S(3) | 2.36(1) | Ru−S(4) | 2.38(1) |
| Ir···Ru | 3.588(5) | Ir···Re(2) | 3.563(3) |

(b) Bond Angles (deg)

| | | | |
|---|---|---|---|
| S(1)−Ir−S(3) | 100.6(5) | S(1)−Ir−S(4) | 79.8(5) |
| S(3)−Ir−S(4) | 80.1(4) | S(1)−Re(1)−S(2) | 99.3(5) |
| S(1)−Re(1)−S(3) | 103.1(5) | S(1)−Re(1)−S(5) | 153.3(6) |
| S(1)−Re(1)−S(6) | 83.0(5) | S(2)−Re(1)−S(3) | 103.6(5) |
| S(2)−Re(1)−S(5) | 80.8(5) | S(2)−Re(1)−S(6) | 144.4(6) |
| S(3)−Re(1)−S(5) | 102.8(6) | S(3)−Re(1)−S(6) | 110.5(6) |
| S(5)−Re(1)−S(6) | 82.0(6) | S(1)−Re(2)−S(2) | 102.6(5) |
| S(1)−Re(2)−S(4) | 80.2(5) | S(1)−Re(2)−S(7) | 142.7(5) |
| S(1)−Re(2)−S(8) | 88.1(5) | S(2)−Re(2)−S(4) | 104.4(5) |
| S(2)−Re(2)−S(7) | 114.7(5) | S(2)−Re(2)−S(8) | 105.6(6) |
| S(4)−Re(2)−S(7) | 88.9(5) | S(4)−Re(2)−S(8) | 149.6(6) |
| S(7)−Re(2)−S(8) | 83.6(6) | S(2)−Ru−S(3) | 100.8(5) |
| S(2)−Ru−S(4) | 101.5(5) | S(3)−Ru−S(4) | 79.8(5) |

geometry around Pd in **13** is severely distorted tetrahedral and that of Ru in **14′** is a three-legged piano stool.

Among the three Re−$S_{sulfide}$ bond lengths around the square pyramidal Re(1) in **13**, the Re(1)−S(3) distance (2.205(4) Å) is shorter than the other two (Re(1)−S(1), 2.327(4); Re(1)−S(2), 2.391(4) Å) and four S(3)−Re−S angles are all obtuse. Hence, the S(3) atom bridging Re(1) and two heterometals can be assigned as the apical S atom as in **2** and **4**. As for the $S_{apical}$−Re−S angles around Re(1), the S(3)−Re(1)−S(1) and S(3)−Re(1)−S(2) angles are analogous to each other at 104.5(1)° and 106.9(1)°, whereas

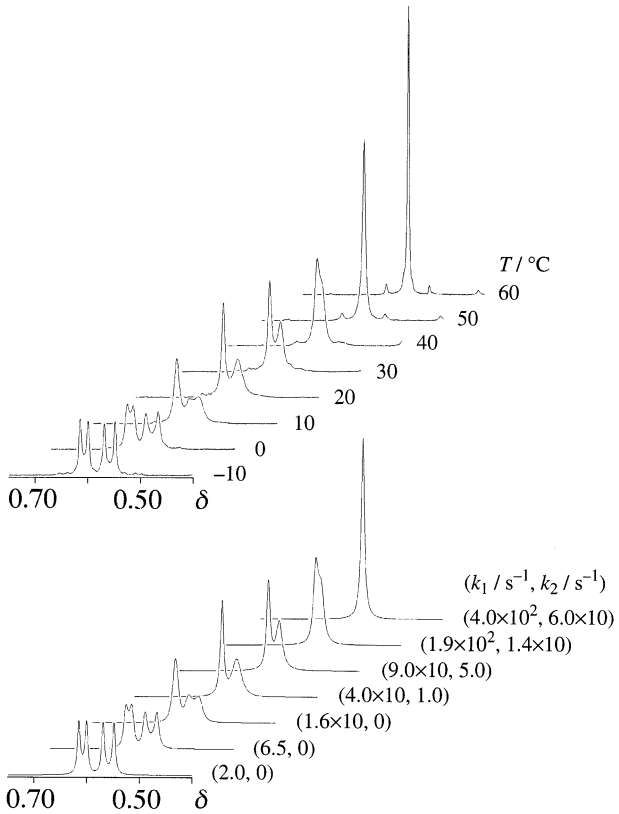


**Figure 7.** The $SiMe_3$ resonances in the variable-temperature $^1H$ NMR spectra for **13** (upper) and their simulated curves (lower) using the $k_1$ and $k_2$ values shown in parentheses. The $k_1$ and $k_2$ values related to the exchange processes are shown in Scheme 5.

the S(3)−Re(1)−S(5) and S(3)−Re(1)−S(6) angles of 98.6(2)° and 109.5(2)° differ considerably. With respect to Re(2), the apical S atom corresponds not to S(4) but to S(2), which bridges heteroatom Pd and Re(1) in addition to Re(2), since the Re(2)−S(2) bond length of 2.245(4) Å is apparently shorter than the Re(2)−S(1) and Re(2)−S(4) bond distances at 2.328(4) and 2.343(4) Å, respectively, and all S(2)−Re(2)−S angles are obtuse: 105.4(1)°, 110.3(1)°, 104.0(1)°, and 115.2(2)° for the S(2)−Re(2)−S(1), S(2)−Re(2)−S(4), S(2)−Re(2)−S(7), and S(2)−Re(2)−S(8) linkages, respectively. This leads to the most significant difference observed for the structure of **13** from that of the $M_2Re_2$ cubane-type clusters **2** and **4**, viz., the two dithiolene planes in **2** and **4** are bound to the Re centers symmetrically or almost symmetrically with respect to the pseudo mirror plane that bisects the Re−Re vector, whereas these two planes in **13** are twisted by ca. 60° along the Re−Re vector.

In **14′**, the apical sulfide around Re(1) is S(3) with the Re(1)−S(3) bond length at 2.24(1) Å, while that around Re(2) corresponds to S(2) with the same Re−S bond distance (2.24(1) Å). Other four Re−$S_{sulfido}$ bonds are apparently longer than these, and their distances fall in the range 2.34(1)−2.37(1) Å. The other metrical parameters and structural features associated with Re−S bonds in **14′** are analogous to those in **13**. Thus, with respect to the Re atoms in all of the crystallographically analyzed cubane-type clusters **2**, **4**, **13**, and **14′**, all Re atoms have a square pyramidal geometry with one of the three sulfides at the apical position, where

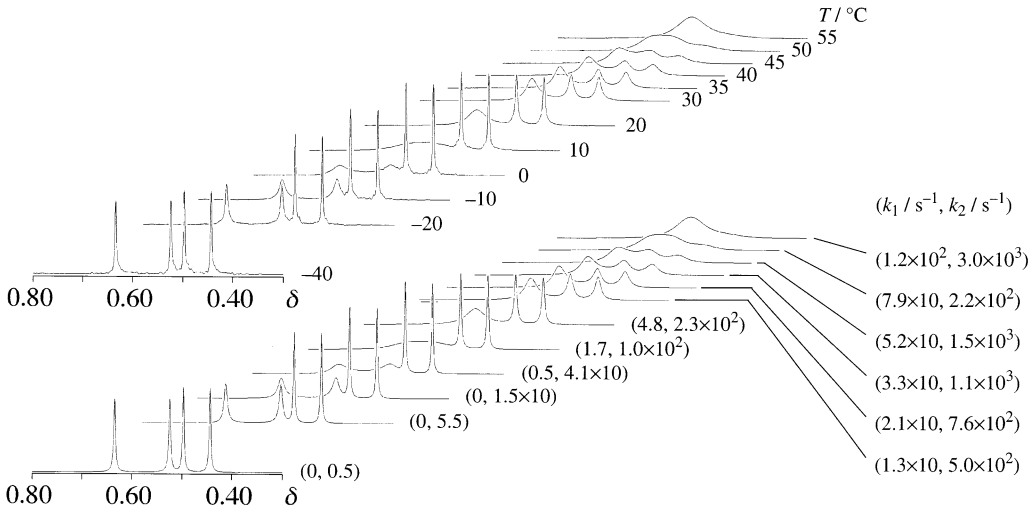


**Figure 8.** The $SiMe_3$ resonances in the variable-temperature $^1H$ NMR spectra for **14** (upper) and their simulated curves (lower) using the $k_1$ and $k_2$ values shown in parentheses. The $k_1$ and $k_2$ values related to the exchange processes are shown in Scheme 5.

the apical sulfide atom of the given Re is assignable to that which bridges both of the two Re−metal single bonds around this Re.

**Variable-Temperature NMR Study for Trimetallic Cubane-Type and Incomplete Cubane-Type Clusters.** The X-ray analyses for **2** and **4** have disclosed that the two dithiolene ligands in these bimetallic cubane-type clusters are equivalent or pseudo equivalent and the two $SiMe_3$ groups in one dithiolene ligand are also nearly equivalent. Hence, the $^1H$ NMR spectra of **2** and **4** exhibiting the $SiMe_3$ signal as one sharp singlet are consistent with their solid-state structures.

In the trimetallic cubane-type clusters **13** and **14′**, four $SiMe_3$ groups are inequivalent in a solid state as demonstrated by the X-ray diffraction, but their signals recorded in $C_6D_6$ at room temperature are quite broad. Thus, further $^1H$ NMR study was carried out for these trimetallic cubane-type clusters to clarify their dynamic behavior in solution.

The variable-temperature $^1H$ NMR spectra of the $SiMe_3$ signal's region for **13** and **14** are shown in Figures 7 and 8. These clearly show that at sufficiently low temperatures the four $SiMe_3$ groups are mutually inequivalent for both clusters as observed in the single-crystal X-ray structures. Interestingly, Figures 7 and 8 also show that the spectral changes occur in different manners. Thus, in the spectra for **13**, four signals observed at low temperatures are first converted into two signals with the same intensity and then coalesce to one resonance upon warming. On the other hand, the spectra for **14** show that among the four signals recorded at the slow exchange limit only two unite initially to give a set of three signals with the intensity ratio of 2:1:1, which coalesce to one resonance at the higher temperatures. In these clusters, equivalency of the $SiMe_3$ groups on the NMR time scale can arise from two processes as shown in Scheme 5; one is the rapid exchange of the two Re centers due to the migration of the Re−heterometal bond, the other being the fast pseudo-roatation of the dithiolene ligand around the pentacoordinate Re atom. The spectral change of the given clusters may be determined by the difference in the activation energies of these processes for each cluster. It is to be noted that the dynamic process of the cubane-type core attributable to the migration of the metal−metal bond has previously been reported for the clusters $[\{(MeCp)Ru\}_4(\mu_3\text{-}S)_4]^{2+}$,[24] $[(Cp^*Ir)_4(\mu_3\text{-}S)_4]^{2+}$,[25] and $[CpTi(Cp^*Ru)_3(\mu_3\text{-}S)_4]$.[10]

The spectral change for **13** may be explained by the coalescence process involving the exchange of the two Re sites prior to the rotation of the dithiolene ligand. Thus, one extreme structure of **13** containing four inequivalent $SiMe_3$ groups can be described as **i** in Scheme 5, which is rigid, and the rearrangement to the equivalent structure **ii** is slow enough in the NMR time scale at low temperatures. Upon warming, migration of the Re−Ir bond occurs first, which is accompanied by the rearrangement of the apical Re−S bond as well as the orientation of the basal plane, affording **ii**. Rapid interconversion between **i** and **ii** results in the coalescence of the signals of two $SiMe_3$ groups: $\delta(A) = \delta(C)$ and $\delta(B) = \delta(D)$. When the temperature is raised further, facile rotation of the ditiolene ligand around Re also becomes possible, which makes the four $SiMe_3$ groups equivalent in the NMR criteria.

In contrast, for **14** the rotation of the dithiolene ligand is presumed to take place more readily. Thus, by interconversion between **i** and **iii** coalescence of only the two signals assignable to A and B in **i** is observed first. At higher temperatures, the Re−Ir bond migration also occurs rapidly, whereby the $SiMe_3$ groups are recorded as only one singlet. The activation energies, $\Delta G_1^{\ddagger}$ and $\Delta G_2^{\ddagger}$, which have proved essentially unaffected by the temperature range, are calculated from the $^1H$ NMR spectra by the line-shape analyses to be $62.7 \pm 0.8$ and $69.3 \pm 1.4$ kJ·mol$^{-1}$ for **13** (Figure 7) and $67.7 \pm 0.6$ and $58.4 \pm 0.7$ kJ·mol$^{-1}$ for **14** (Figure 8), respectively. As summarized in Table 6, the spectral change consistent with the order of the activation energies $\Delta G_1^{\ddagger} < \Delta G_2^{\ddagger}$ for **13** was also observed for **9** and that interpreted by the order $\Delta G_1^{\ddagger} > \Delta G_2^{\ddagger}$ for **14** occurs in the spectra of **15**,

(24) Houser, E. J.; Amarasekera, J.; Rauchfuss, T. B.; Wilson, S. R. *J. Am. Chem. Soc.* **1991**, *113*, 7440.
(25) Venturelli, A.; Rauchfuss, T. B. *J. Am. Chem. Soc.* **1994**, *116*, 4824.

**Scheme 5**

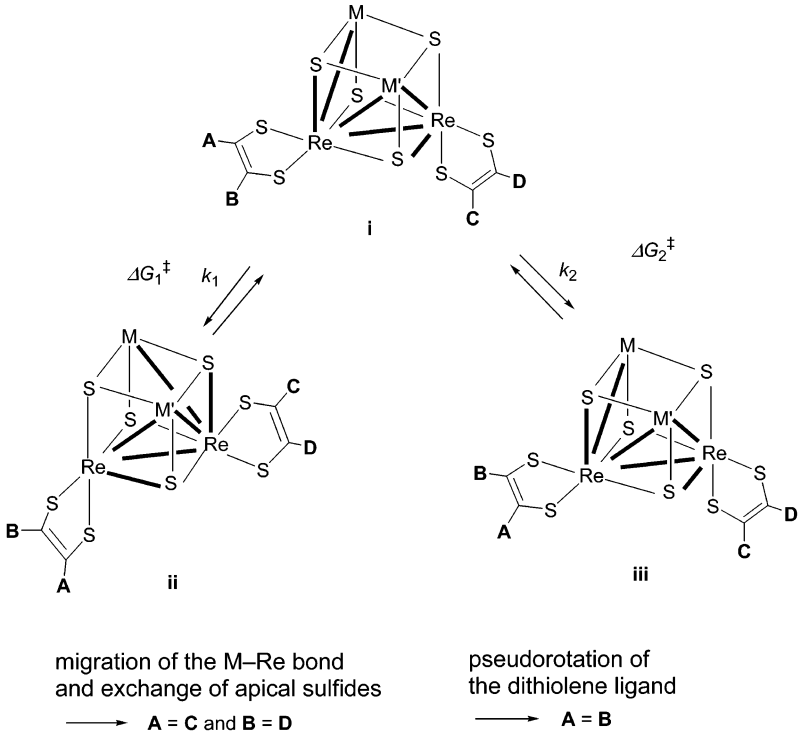


**Table 6.** Activation Parameters Estimated from the Signal Exchange Rates for Incomplete Cubane-Type and Trimetallic Cubane-Type Clusters[a]

| cluster | $\Delta G_1^{\ddagger}$ kJ·mol$^{-1}$ | $\Delta H_1^{\ddagger}$ kJ·mol$^{-1}$ | $\Delta S_1^{\ddagger}$ J·mol$^{-1}$·K$^{-1}$ | $\Delta G_2^{\ddagger}$ kJ·mol$^{-1}$ | $\Delta H_2^{\ddagger}$ kJ·mol$^{-1}$ | $\Delta S_2^{\ddagger}$ J·mol$^{-1}$·K$^{-1}$ |
|---|---|---|---|---|---|---|
| **5** | 53.6 ± 1.0 | 46 ± 3 | −29 ± 10 | 66.6 ± 1.2 | *b* | *b* |
| | (223−283) | (243−283) | | (303−323) | | |
| **6** | 50.4 ± 0.6 | 52 ± 2 | 6 ± 8 | 69.6 ± 0.9 | 65 ± 5 | −15 ± 13 |
| | (223−273) | (223−273) | | (313−363) | (323−363) | |
| **7** | 60.1 ± 0.7 | 59 ± 3 | −5 ± 11 | 68.5 ± 0.6 | 64 ± 4 | −12 ± 10 |
| | (253−293) | (253−293) | | (313−363) | (313−363) | |
| **9** | 50.3 ± 0.7 | 47 ± 2 | −16 ± 9 | 57.6 ± 0.7 | 58 ± 3 | 0 ± 12 |
| | (213−253) | (213−253) | | (263−303) | (263−303) | |
| **10** | 53.0 ± 0.6 | 49 ± 5[c] | −16 ± 20[c] | 54.7 ± 0.6 | 54 ± 3 | −2 ± 14 |
| | (243−263) | (243−263) | | (233−263) | (233−263) | |
| **11** | 54.8 ± 0.6 | 55 ± 4 | 1 ± 14 | 56.1 ± 0.7 | 53 ± 3 | −14 ± 10 |
| | (243−273) | (243−273) | | (233−273) | (233−273) | |
| **13**[d] | 62.7 ± 0.8 | 58 ± 4 | −16 ± 15 | 69.3 ± 1.4 | *b* | *b* |
| | (273−303) | (273−303) | | (303−323) | | |
| **14**[e] | 67.7 ± 0.6 | 71 ± 7[c] | 10 ± 21[c] | 58.4 ± 0.7 | 56 ± 2 | −9 ± 8 |
| | (303−323) | (303−323) | | (233−313) | (253−313) | |
| **15** | 70.2 ± 1.2 | 68 ± 4 | −5 ± 13 | 64.7 ± 0.8 | 63 ± 3 | −7 ± 12 |
| | (283−343) | (303−343) | | (263−303) | (263−303) | |

[a] In toluene-$d_8$. Temperature ranges in K used for determining the parameters are in parentheses. [b] Values were unavailable since good linear correlations could not be observed. [c] Determined by only three data. [d] In toluene-$d_8$−$C_6D_6$ (1:1). [e] In THF-$d_8$.

whereas the $\Delta G_1^{\ddagger}$ and $\Delta G_2^{\ddagger}$ values for **10** and **11** are calculated to be very close.

In the incomplete cubane-type **7**, although two dithiolene ligands are crystallographically equivalent, two $SiMe_3$ groups in one dithiolene ligand are apparently nonequivalent. Consistently, the $^1$H NMR spectrum of **7** in $C_6D_6$ at room temperature showed two singlets due to the $SiMe_3$ protons

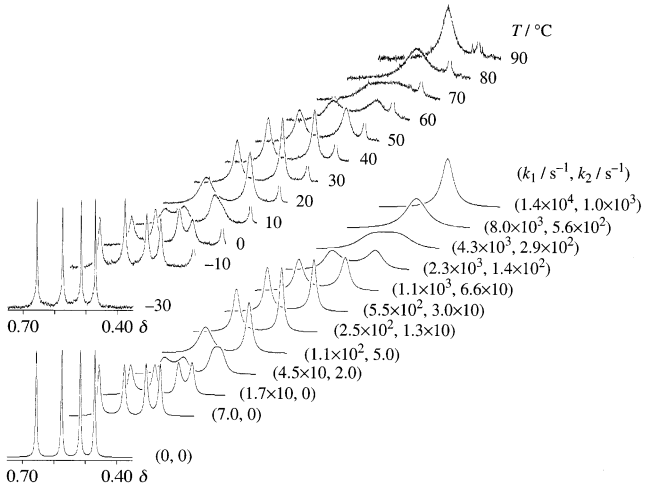


**Figure 9.** The $SiMe_3$ resonances in the variable-temperature $^1$H NMR spectra for **7** (upper) and their simulated curves (lower) using the $k_1$ and $k_2$ values shown in parentheses. The $k_1$ and $k_2$ values related to the exchange processes are shown in Scheme 6.

with the same intensity; however, these signals were somehow broadened significantly. Hence the variable-temperature $^1$H NMR study has also been undertaken for **7**. Figure 9 shows that the limiting low-temperature spectrum exhibits four $SiMe_3$ resonances also for **7**; upon warming, these signals coalesce into two signals with the same intensity, which are then converted into one singlet. This feature analogous to that of **13** can be explained by presuming the presence of essentially the same dynamic processes depicted in Scheme 6, where $\Delta G_1^{\ddagger} < \Delta G_2^{\ddagger}$. The

**Scheme 6**

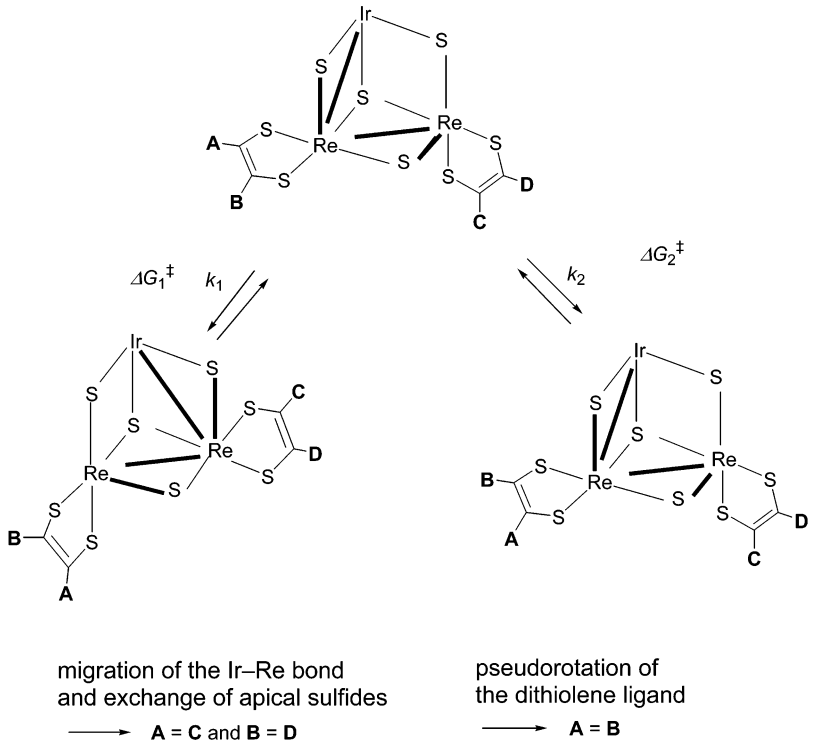


Metal—metal and apical metal—sulfide bonds are shown by thick lines for clarity.

other incomplete cubane-type clusters **5** and **6** also showed similar spectral changes. The symmetrical structure determined by the single-crystal X-ray analysis is probably favored only in a crystalline form because of the packing effect, but the details are currently unknown.

To elaborate on the difference in the order of $\Delta G_1^{\ddagger}$ and $\Delta G_2^{\ddagger}$ depending on the nature of the cubane-type cores along with the relationship between the X-ray structure and the structures in solution for incomplete cubane-type cores, detailed MO calculations will be carried out for a series of the clusters investigated here. Further studies are also in progress to clarify the reactivities of the new trinuclear and tetranuclear clusters toward a variety of small molecules. These results will be reported in due course.

## Experimental Section

**General.** All manipulations were carried out under $N_2$ using standard Schlenk tecniques. Solvents were dried by common procedures and distilled under $N_2$ before use. Complexes **1**,[19] $[(Cp^*Ru)_4(\mu_3\text{-}Cl)_4]$,[26] $[(PtMe_3)_4(\mu_3\text{-}I)_4]$,[27] $[\{Cu(PPh_3)\}_4(\mu_3\text{-}Cl)_4]$,[28] $[(Cp^*MCl)_2(\mu\text{-}Cl)_2]$ (M = Rh, Ir),[29] $[M(CO)_3(MeCN)_3]$ (M = Mo, W),[30] $[Pd(PPh_3)_4]$,[31] $[Cp^*Ru(MeCN)_3][PF_6]$,[32] and $[\{Rh(cod)\}_2(\mu\text{-}Cl)_2]$[33] were prepared according to the literature methods, while the synthesis of $[\{(\eta^6\text{-}C_6HMe_5)RuCl\}_2(\mu\text{-}Cl)_2]$ was done as described for its $C_6Me_6$ analogue.[34] Other reagents were commercially obtained and used as received.

NMR and IR spectra were measured on a JEOL alpha-400 or a JASCO FT/IR-420 spectrometer, while mass spectra were recorded by a JEOL JMS600H spectrometer. All the NMR data shown below were obtained at room temperature except for those mentioned otherwise. The details in the variable-temperature NMR studies are shown in the text, Figures 7−9, and Table 6, where the line-shape analysis was based on ref 35 and the thermodynamic parameters were determined by the literature methods.[25] Elemental analyses were done with a Perkin-Elmer 2400 series II CHN analyzer.

**Preparation of $[(Cp^*Ru)_2(ReL)_2(\mu_3\text{-}S)_4]$ (2).** A mixture of **1** (90 mg, 0.055 mmol) and $[(Cp^*Ru)_4(\mu_3\text{-}Cl)_4]$ (30 mg, 0.027 mmol) in MeCN (5 mL) was stirred overnight at room temperature. The resulting dark green solid was filtered off, washed with MeCN, and extracted with benzene. The extract was evaporated to dryness under reduced pressure, and the residue was redissolved in a minimum amount of THF. Addition of MeCN afforded **2** as dark green crystals, which were efflorescent and lost all solvating molecules when dried in vacuo (46 mg, 58% yield). $^1$H NMR ($C_6D_6$): $\delta$ 0.57 (s, 36H, $SiMe_3$), 1.96 (s, 30H, Cp*). Anal. Calcd for $C_{36}H_{66}Si_4S_8Ru_2Re_2$: C, 29.98; H, 4.61. Found: C, 30.13; H, 4.67.

(26) Fagan, P. J.; Ward, M. D.; Calabrese, J. C. *J. Am. Chem. Soc.* **1989**, *111*, 1698.
(27) Baldsin, J. C.; Kaska, W. C. *Inorg. Chem.* **1975**, *14*, 2020.
(28) Jardine, F. H.; Vohra, A. G. *J. Chem. Soc. A* **1970**, 238.
(29) White, C.; Yates, A.; Maitlis, P. M. *Inorg. Synth.* **1992**, *29*, 228.
(30) Tate, P.; Knipple, W. R.; Augl, J. M. *Inorg. Chem.* **1962**, *1*, 433.
(31) Coulson, D. R. *Inorg. Synth.* **1972**, *13*, 121.
(32) Steinmetz, B.; Schenk, W. A. *Organometallics* **1999**, *18*, 943.
(33) Giordano, G.; Crabtree, R. H. *Inorg. Synth.* **1979**, *19*, 218.
(34) Bennet, M. A.; Huang, T.-N.; Matheson, T. W.; Smith, A. K. *Inorg. Synth.* **1982**, *21*, 74.
(35) *gNMR: Program for Simulation of One-Dimensional NMR Spectra*; Adept Scientific: Amor Way, U.K., 1995−1999.

The following compounds were prepared by essentially the same method.

**[(PtMe$_3$)$_2$(ReL)$_2$($\mu_3$-S)$_4$] (3):** dark brown crystals in 26% yield from **1** (84 mg, 0.051 mmol) and [(PtMe$_3$)$_4$($\mu_3$-I)$_4$] (38 mg, 0.026 mmol). $^1$H NMR ($C_6D_6$): $\delta$ 0.44 (s, 36H, SiMe$_3$), 2.09 (s with $^{195}$Pt satellites, $J_{Pt-H}$ = 74.2 Hz, 12H, PtMe), 2.50 (s with $^{195}$Pt satellites, $J_{Pt-H}$ = 69.8 Hz, 6H, PtMe). Anal. Calcd for $C_{22}H_{54}Si_4S_8Pt_2Re_2$: C, 18.22; H, 3.75. Found: C, 18.56; H, 3.84.

**[{Cu(PPh$_3$)}$_2$(ReL)$_2$($\mu_3$-S)$_4$] (4):** dark brown crystals in 68% yield from **1** (83 mg, 0.050 mmol) and [{Cu(PPh$_3$)}$_4$($\mu_3$-Cl)$_4$] (37 mg, 0.026 mmol). $^1$H NMR ($C_6D_6$): $\delta$ 0.51 (s, 36H, SiMe$_3$), 7.1−7.3 (m, 18H, Ph), 7.8−8.0 (m, 12H, Ph). $^{31}$P{$^1$H} NMR ($C_6D_6$): $\delta$ −6.5 (br). Anal. Calcd for $C_{52}H_{66}Si_4P_2S_8Cu_2Re_2$: C, 38.52; H, 4.10. Found: C, 39.06; H, 4.30.

**[{($\eta^6$-C$_6$Me$_5$H)Ru}(ReL)$_2$($\mu_3$-S)($\mu_2$-S)$_3$] (5).** A mixture containing **1** (332 mg, 0.202 mmol) and [{($\eta^6$-C$_6$HMe$_5$)RuCl}$_2$($\mu$-Cl)$_2$] (66 mg, 0.10 mmol) in MeCN (5 mL) was stirred overnight at room temperature. A brown solid precipitated, which was filtered off, washed with MeCN, and extracted with benzene. The extract was dried up in vacuo, and the residue was crystallized from THF−MeCN, affording **5**·THF (86 mg, 33%). FAB MS (*m*-nitrobenzyl alcohol, *m*/*z*): 1220 (M$^+$). $^1$H NMR ($C_6D_6$): $\delta$ 0.47, 0.60 (s, 18H each, SiMe$_3$), 1.44, 1.48 (br s, 6H each, C$_6$Me-1,2,4, or 5), 1.65 (s, 3H, C$_6$Me-3), 4.61 (br s, 1H, C$_6$H), 1.41, 3.56 (m, 4H each, THF). Anal. Calcd for $C_{31}H_{60}OSi_4S_8RuRe_2$: C, 28.84; H, 4.68. Found: C, 28.36; H, 4.72.

The following two compounds were prepared in an analogous manner.

**[(Cp*Rh)(ReL)$_2$($\mu_3$-S)($\mu_2$-S)$_3$] (6):** brown crystals in 45% yield from **1** (82 mg, 0.050 mmol) and [(Cp*RhCl)$_2$($\mu$-Cl)$_2$] (16 mg, 0.026 mmol). FAB MS (*m*-nitrobenzyl alcohol, *m*/*e*): 1208 (M$^+$). $^1$H NMR ($C_6D_6$): $\delta$ 0.45, 0.58 (s, 18H each, SiMe$_3$), 1.38 (s, 15H, Cp*). Anal. Calcd for $C_{26}H_{51}Si_4S_8RhRe_2$: C, 25.85; H, 4.26. Found: C, 25.95; H, 4.42.

**[(Cp*Ir)(ReL)$_2$($\mu_3$-S)($\mu_2$-S)$_3$] (7):** brown crystals in 80% yield from **1** (1.09 g, 0.661 mmol) and [(Cp*IrCl)$_2$($\mu$-Cl)$_2$] (265 mg, 0.333 mmol). FAB MS (*m*-nitrobenzyl alcohol, *m*/*z*): 1296 (M$^+$). $^1$H NMR ($C_6D_6$): $\delta$ 0.46, 0.60 (br s, 18H each, SiMe$_3$), 1.39 (s, 15H, Cp*). Anal. Calcd for $C_{26}H_{51}Si_4S_8IrRe_2$: C, 24.07; H, 3.96. Found: C, 24.12; H, 4.07.

**[{($\eta^6$-C$_6$Me$_5$H)Ru}{W(CO)$_3$}(ReL)$_2$($\mu_3$-S)$_4$] (8).** A THF solution (5 mL) containing **5**·THF (52 mg, 0.040 mmol) and [W(CO)$_3$(MeCN)$_3$] (17 mg, 0.044 mmol) was stirred overnight at room temperature, and the resultant dark brown solution was filtered. Addition of MeCN to the concentrated filtrate gave black microcrystals, which were filtered off and dried in vacuo (15 mg, 25% yield). $^1$H NMR ($C_6D_6$): $\delta$ 0.52 (br s, 36H, SiMe$_3$), 1.30 (br, 9H, C$_6$Me), 1.35 (br, 6H, C$_6$Me), 4.33 (s, 1H, C$_6$H). IR (KBr) $\nu$(C≡O): 1997, 1954, 1890 cm$^{-1}$. Anal. Calcd for $C_{30}H_{52}O_3Si_4S_8RuWRe_2$: C, 24.23; H, 3.52. Found: C, 24.31; H, 3.88.

The following compounds were prepared similarly.

**[(Cp*Rh){W(CO)$_3$}(ReL)$_2$($\mu_3$-S)$_4$] (9):** brown microcrystals in 23% yield from **6** (25 mg, 0.021 mmol) and [W(CO)$_3$(MeCN)$_3$] (8.2 mg, 0.021 mmol). FAB MS (*m*-nitrobenzyl alcohol, *m*/*z*): 1476 (M$^+$). $^1$H NMR ($C_6D_6$): $\delta$ 0.50 (br s, 36H, SiMe$_3$), 1.14 (s, 15H, Cp*). IR (KBr) $\nu$(C≡O): 2004, 1961, 1899 cm$^{-1}$. Anal. Calcd for $C_{29}H_{51}O_3Si_4S_8RhWRe_2$: C, 23.60; H, 3.48. Found: C, 23.97; H, 3.58.

**[(Cp*Ir){W(CO)$_3$}(ReL)$_2$($\mu_3$-S)$_4$] (10):** dark brown crystals of **10**·$^1/_2$MeCN in 26% yield from **7** (33 mg, 0.025 mmol) and [W(CO)$_3$(MeCN)$_3$] (9.7 mg, 0.025 mmol). $^1$H NMR ($C_6D_6$): $\delta$ 0.51 (br s, 36H, SiMe$_3$), 1.16 (s, 15H, Cp*), 1.54 (s, 1.5H, MeCN). IR (KBr) $\nu$(C≡O): 2002, 1959, 1898 cm$^{-1}$. Anal. Calcd for $C_{30}H_{52.5}N_{0.5}O_3Si_4S_8IrWRe_2$: C, 22.73; H, 3.34; N, 0.44. Found: C, 22.91; H, 3.61; N, 0.40.

**[(Cp*Ir){Mo(CO)$_3$}(ReL)$_2$($\mu_3$-S)$_4$] (11):** dark brown microcrystals of **11**·$^1/_2$THF in 59% yield from **7** (66 mg, 0.051 mmol) and [Mo(CO)$_3$(MeCN)$_3$] (20 mg, 0.067 mmol). $^1$H NMR ($C_6D_6$): $\delta$ 0.51 (br s, 36H, SiMe$_3$), 1.17 (s, 15H, Cp*), 1.41, 3.56 (m, 2H each, THF). IR (KBr) $\nu$(C≡O): 2007, 1968, 1908 cm$^{-1}$. Anal. Calcd for $C_{31}H_{55}O_{3.5}Si_4S_8IrMoRe_2$: C, 24.61; H, 3.66. Found: C, 24.26; H, 3.82.

**[{($\eta^6$-C$_6$HMe$_5$)Ru}{Pd(PPh$_3$)}(ReL)$_2$($\mu_3$-S)$_4$] (12):** black crystals in 57% yield from **5** (58 mg, 0.048 mmol) and [Pd(PPh$_3$)$_4$] (57 mg, 0.049 mmol). $^1$H NMR ($C_6D_6$): $\delta$ 0.54, 0.58 (br s, 18H each, SiMe$_3$), 1.38 (br s, 9H, C$_6$Me), 1.47 (s, 6H, C$_6$Me), 4.55 (s, 1H, C$_6$H), 7.1−7.3 (m, 9H, Ph), 7.9−8.0 (m, 6H, Ph). $^{31}$P{$^1$H} NMR ($C_6D_6$): $\delta$ 46.2 (s). Anal. Calcd for $C_{45}H_{67}Si_4PS_8RuPdRe_2$: C, 34.04; H, 4.25. Found: C, 33.96; H, 4.34.

**[(Cp*Ir){Pd(PPh$_3$)}(ReL)$_2$($\mu_3$-S)$_4$] (13):** dark brown crystals in 63% yield from **7** (250 mg, 0.193 mmol) and [Pd(PPh$_3$)$_4$] (224 mg, 0.194 mmol). $^1$H NMR ($C_6D_6$): $\delta$ 0.54, 0.57 (br s, 18H each, SiMe$_3$), 1.28 (s, 15H, Cp*), 7.1−7.3 (m, 9H, Ph), 7.9−8.0 (m, 6H, Ph). $^{31}$P{$^1$H} NMR ($C_6D_6$): $\delta$ 52.6 (s). Anal. Calcd for $C_{44}H_{66}Si_4PS_8IrPdRe_2$: C, 31.72; H, 3.99. Found: C, 31.91; H, 4.15.

**[(Cp*Ir)(Cp*Ru)(ReL)$_2$($\mu_3$-S)$_4$][PF$_6$] (14).** This complex was obtained from **7** (65 mg, 0.050 mmol) and [Cp*Ru(MeCN)$_3$][PF$_6$] (25 mg, 0.049 mmol) by addition of diethyl ether to the concentrated product solution in THF. Brown crystals in 83% yield (69 mg). FAB MS (*m*-nitrobenzyl alcohol, *m*/*z*): 1533 (cation). $^1$H NMR ($C_6D_6$): $\delta$ 0.4−0.55 (br, 36H, SiMe$_3$), 1.54, 1.75 (s, 15H each, Cp*). IR (KBr) $\nu$(P−F): 841 cm$^{-1}$. Anal. Calcd for $C_{36}H_{66}F_6PSi_4S_8IrRuRe_2$: C, 25.76; H, 3.96. Found: C, 25.94; H, 4.02.

**[(Cp*Ir)(Cp*Ru)(ReL)$_2$($\mu_3$-S)$_4$][SbF$_6$] (14′).** A mixture of **14** (30 mg, 0.018 mmol) and Na[SbF$_6$] (34 mg, 0.13 mmol) in THF (5 mL) was stirred at room temperature for 18 h. The resulting mixture was evaporated to dryness, and the residue was extracted with benzene. The extract was dried up again and crystallized from THF−diethyl ether, affording **14′** as the brown efflorescent crystals quantitatively. The crystals obtained were thoroughly dried under vacuum at room temperature. $^1$H NMR ($C_6D_6$): $\delta$ 0.4−0.55 (br, 36H, SiMe$_3$), 1.51, 1.73 (s, 15H each, Cp*). Anal. Calcd for $C_{36}H_{66}F_6Si_4S_8SbIrRuRe_2$: C, 24.44; H, 3.76. Found: C, 24.52; H, 3.78.

**[(Cp*Ir){Rh(cod)}(ReL)$_2$($\mu_3$-S)$_4$][PF$_6$] (15).** A mixture of **10** (65 mg, 0.050 mmol), [{Rh(cod)}$_2$($\mu$-Cl)$_2$] (13 mg, 0.026 mmol), and K[PF$_6$] (19 mg, 0.10 mmol) in THF (5 mL) was stirred at room temperature for 22 h. The resulting mixture was evaporated to dryness, and the residue was extracted with benzene. The extract was dried up again and crystallized from THF−diethyl ether. The yield of the dark brown crystals of **15**·0.5Et$_2$O was 61 mg (72% yield). FAB MS (*m*-nitrobenzyl alcohol, *m*/*z*): 1507 (cation). $^1$H NMR ($C_6D_6$): $\delta$ 0.44, 0.53 (br, 9H each, SiMe$_3$), 0.48, 0.51 (s, 9H each, SiMe$_3$), 1.10 (t, 3H, diethyl ether), 1.66 (s, 15H, Cp*), 3.25 (q, 2H, diethyl ether). The signals assigned to the cod protons by recording at −40 °C are as follows (toluene-$d_8$): $\delta$ 1.25−1.4 (m, 2H each), 2.25−2.4, 2.45−2.55, 3.15−3.3 (m, 1H each), 3.35−3.6 (m, 2H), 4.15−4.25, 6.4−6.5, 6.5−6.6 (m, 1H each). IR (KBr) $\nu$(P−F): 841 cm$^{-1}$. Anal. Calcd for $C_{36}H_{68}O_{0.5}F_6PSi_4S_8IrRhRe_2$: C, 25.58; H, 4.05. Found: C, 25.62; H, 4.05.

**X-ray Crystallography.** Single crystals of **4**, **7**, and **13** were sealed in glass capillaries under Ar and subjected to the X-ray diffraction studies, while the crystals of **2** and **14′** were sealed together with mother liquor of recrystallization (THF−MeCN or THF−ether) to avoid decay. All diffraction studies were carried out on a Rigaku AFC7R diffractometer equipped with a graphite-

**Table 7.** Crystallographic Data for **2**, **4**, **7**, **13**, and **14′**

| | **2**·1.375MeCN | **4** | **7** | **13** | **14′**·2THF |
|---|---|---|---|---|---|
| formula | $C_{38.75}H_{70.125}N_{1.375}Si_4S_8Ru_2Re_2$ | $C_{52}H_{66}Si_4P_2S_8Cu_2Re_2$ | $C_{26}H_{51}Si_4S_8Re_2Ir$ | $C_{44}H_{66}Si_4PS_8PdRe_2Ir$ | $C_{44}H_{84}O_2F_6Si_4SbS_8RuRe_2Ir$ |
| fw | 1498.74 | 1621.37 | 1311.17 | 1665.84 | 1913.40 |
| space group | $R\bar{3}$ (No. 148) | $C2/c$ (No.15) | $Cmc2_1$ (No. 36) | $P2_1/c$ (No. 14) | $Pccn$ (No. 56) |
| $a$ (Å) | 41.896(4) | 24.486(3) | 35.144(7) | 16.758(4) | 20.032(2) |
| $b$ (Å) | 41.896(4) | 11.31(1) | 9.422(2) | 20.207(4) | 45.488(4) |
| $c$ (Å) | 34.890(10) | 24.036(3) | 12.975(5) | 19.476(2) | 15.938(2) |
| α (deg) | 90 | 90 | 90 | 90 | 90 |
| $\beta$ (deg) | 90 | 98.00(1) | 90 | 105.88(1) | 90 |
| $\gamma$ (deg) | 120 | 90 | 90 | 90 | 90 |
| $V$ (Å$^3$) | 53035(15) | 6591(8) | 4297(2) | 6343(1) | 14523(2) |
| $Z$ | 36 | 4 | 4 | 4 | 8 |
| $\rho_{calc}$ (g cm$^{-3}$) | 1.689 | 1.634 | 2.005 | 1.744 | 1.750 |
| $F$(000) | 26433 | 3200 | 2472 | 3208 | 7392 |
| $\mu_{calc}$ (cm$^{-1}$) | 49.90 | 47.05 | 92.39 | 65.73 | 60.65 |
| cryst size (mm) | 1.0 × 0.8 × 0.4 | 0.2 × 0.2 × 0.15 | 0.3 × 0.2 × 0.05 | 0.5 × 0.1 × 0.03 | 0.55 × 0.5 × 0.2 |
| scan type | $\omega$ | $\omega$ | $\omega$ | $\omega-2\theta$ | CCD |
| 2$\theta$ range (deg) | 5−50 | 5−55 | 5−55 | 5−55 | 6−55 |
| no. of unique reflns | 20706 | 7580 | 5307 | 14546 | 16512 |
| no. of obsd reflns ($I > 3\sigma(I)$) | 11382 | 4512 | 3350 | 5505 | 7896 |
| no. of variables | 927 | 316 | 223 | 551 | 673 |
| transmn factor | 0.61−1.00 | 0.84−1.00 | 0.52−1.00 | 0.79−1.00 | 0.38−1.00 |
| R1 | 0.063 | 0.039 | 0.039 | 0.041 | 0.060 |
| wR1 or wR2 | wR1 = 0.071 | wR1 = 0.035 | wR2 = 0.102 | wR1 = 0.042 | wR2 = 0.145 |
| GOF | 1.99 | 1.31 | 1.02 | 1.26 | 1.00 |
| largest peak/hole (e Å$^{-3}$) | 3.69/−1.99 | 1.16/−1.47 | 1.93/−1.67 | 1.00/−0.92 | 1.66/−1.45 |

monochromatized Mo Kα source except for that of **14′**, which was done on a Rigaku Mercury CCD area detector. Details are shown in Table 7.

Structure solution and refinements were performed by using the *teXsan* program package[36] for **2**, **4**, and **13** or *CrystalStructure* program package[37] for **7** and **14′**. The positions of the non-hydrogen atoms were determined by Patterson methods (PATTY[38] for **2**, **4**, **7**, and **13** or SHELXS97[39] for **14′**), followed by Fourier synthesis (DIRDIF 94[40] for **2**, **4**, and **13** or DIRDIF99[41] for **7** and **14′**). These were refined anisotropically by using full-matrix least-squares techniques. The hydrogen atoms were placed at the calculated positions and included in the final stages of the refinements with fixed parameters.

For **2**, the carbon atoms in one Cp* ligand and one $SiMe_3$ group in molecule 2 were each located at two disordered positions with occupancies of 0.6 and 0.4 for the former and 0.5 and 0.5 for the latter. The Cp* carbon atoms in the major component were refined isotropically, while those in the minor component were treated as the rigid group. The disordered carbon atoms in the $SiMe_3$ group were refined isotropically. The absolute structure for **7** was validated by refinement of Flack parameter $\chi$, which converged to 0.00(2).

In **14′**, both Cp* ligands are shown to have two disordered orientations with the occupancy ratio 0.6:0.4. The Cp* C atoms of the minor component were refined only isotropically. For the solvating THF molecules, all non-hydrogen atoms were refined with restraints with isotropic thermal parameters.

The X-ray analysis was done also for **3**. Crystal data are as follows: $a = 9.506(6)$ Å, $b = 13.360(3)$ Å, $c = 33.968(5)$ Å, $\beta = 91.59(3)°$, $V = 4344(3)$ Å$^3$, $Z = 4$ in space group $P2_1/n$ (No. 14). The atom connecting scheme has been confirmed, but the $R$ value did not converge to the acceptable level because of the poor quality of the crystal.

**Acknowledgment.** We are grateful to Dr. Izuru Takei of the University of Tokyo for the X-ray diffraction study of **7**. This work was supported by a Grant-in-Aid for Scientific Research on Priority Areas (No. 14078206, "Reaction Control of Dynamic Complexes") from the Ministry of Education, Culture, Sports, Science and Technology, Japan, and by CREST of JST (Japan Science and Technology Corporation).

**Supporting Information Available:** Tables of crystallographic data and crystallographic data in CIF format for **2**, **4**, **7**, **13**, and **14′**. This material is available free of charge via the Internet at http://pubs.acs.org.

IC030129K

(36) *teXsan: Crystal Structure Analysis Package*; Molecular Structure Corp.: The Woodlands, TX, 1985 and 1992.

(37) *CrystalStructure 3.00: Crystal Structure Analysis Package*; Rigaku and Rigaku/MSC: 2000−2002. *CRYSTALS* Issue 10: Watkin, D. J.; Prout, C. K.; Carruthers, J. R.; Betteridge, P. W. Chemical Crystallography Laboratory: Oxford, U.K..

(38) PATTY: Beurskens, P. T.; Admiraal, G.; Beurskens, G.; Bosman, W. P.; Garcia-Granda, S.; Gould, R. O.; Smits, J. M. M.; Smykall, C. *The DIRDIF program system*; Technical Report of the Crystallography Laboratory: University of Nijmegen, Nijmegen, The Netherlands, 1992.

(39) SHELX97: Sheldrick, G. M. Program for the Refinement of Crystal Structures: University of Göttingen: Göttingen, Germany.

(40) DIRDIF94: Beurskens, P. T.; Admiraal, G.; Beurskens, G.; Bosman, W. P.; de Gelder, R.; Israel, R.; Smits, J. M. *The DIRDIF-94 program system*; Technical Report of the Crystallography Laboratory: University of Nijmegen, Nijmegen, The Netherlands, 1994.

(41) DIRDIF99: Beurskens, P. T.; Admiraal, G.; Beurskens, G.; Bosman, W. P.; de Gelder, R.; Israel, R.; Smits, J. M. *The DIRDIF-99 program system*; Technical Report of the Crystallography Laboratory: University of Nijmegen, Nijmegen, The Netherlands, 1999.